West Chester University
Digital Commons @ West Chester University

10-1-2015

Electron transfer during metal-assisted and stain etching of silicon

Kurt W. Kolasinski

West Chester University of Pennsylvania, kkolasinski@wcupa.edu

Recommended Citation

Electron transfer during Metal Assisted and Stain Etching of Silicon

Kurt W. Kolasinski

Department of Chemistry, West Chester University, West Chester, PA, 19383-2115 USA

The etching of silicon in fluoride solutions is limited by the kinetics of charge transfer not thermodynamics. This characteristic is what gives fluoride etching its great versatility in making different types of nanostructures as the result of self-limiting chemistry. This review approaches the kinetics of electron transfer from silicon and metal coated silicon to a solution phase species from a fundamental point of view in order to establish a better understanding of the mechanisms of nanostructure formation during metal assisted and stain etching of silicon. Band bending calculations demonstrate that diffusion of holes away from low work function metals such as Ag is not possible. Similarly diffusion of holes outside of the space charge layer is not possible for high work function metals such as Au, Pd and Pt. While direct hole injection may be important for etch track pore formation in the immediate vicinity of the metal, the charge imbalance on or near the metal causes the metal to act like a nanopower supply that polarizes the surrounding Si. This second mechanism is implicated in nonlocal etching of Si during metal assisted etching.

Corresponding Author

kkolasinski@wcupa.edu

Introduction

Porous silicon, most generally defined, is a mixture of solid silicon and void. This general definition allows us to include several interesting classes of materials. Porous silicon can be formed through a wide variety of processes [1]. Traditional porous silicon is a thin film of solid silicon and voids, usually made by anodization. Electroless etching facilitates the formation of such traditional porous silicon thin films [2-4] as well as powders [5]. However, when combined with an array of metal nanoparticles or holes in a metal film, stain etching can produce a forest of nanowires or an array of macropores [4,6-9]. The nanowires can either be solid or porous. The macropores can be surrounded by either solid or porous silicon. This form of stain etching modified by the catalytic action of a metal is called metal assisted etching (MAE). Several other names are associated with this process. The most common is metal assisted chemical etching (MACE). However, since it is essential that the etch mechanism is an electrochemical process and because a purely chemical etch process cannot lead to the formation of mesoporous silicon, I steadfastly refuse to use this acronym.

Peng and co-workers [10-12] were the first to observe silicon nanowire (SiNW) formation with MAE. This group also demonstrated that ordered arrays of nanowires could be formed using nanosphere lithography to pattern the metal catalyst [13]. The discovery that metal assisted etching could produce not only por-Si but also SiNW, especially in ordered arrays has led to a revitalization of electroless Si etching [6,7,14-18]. Importantly, both stain etching and MAE can be used to etch Si stock with any initial morphology: (single-crystal or multicrystalline) wafer, chunk, powder, even microneedles formed by laser ablation (so-called black silicon) [19,20].

In this review it is emphasized that arguments that rely upon thermodynamics are sure to fail in describing the essence of stain etching and MAE. The reason for this is that both of these processes are kinetically controlled not thermodynamically controlled processes. Here we seek to tease out the parameters that are most important for understanding the rate of the electron transfer and ultimately the rate of silicon etching in these two electroless etching processes.

The two processes of stain etching and metal assisted etching are depicted in Fig. 1. Hole injection into the Si valence band is the rate-limiting step in stain etching and metal-assisted etching because a valence band hole is required to initiate etching of Si. Electron transfer is the first step in hole injection. A Si valence band hole is created directly as a result of electron transfer in the case of stain etching. For metal assisted etching, electron transport across the metal leaving a hole in the Si valence band must occur prior to initiation of etching. While the language of holes is used with respect to charge transport in semiconductors (but not metals), one should keep in mind that holes are not physical particles. They are only mathematical and linguistic constructs that mimic the multi-particle dynamics of electrons. It is always the electrons that move in charge transfer. Therefore, in order to understand the kinetics of stain

etching, we need only an understanding of the kinetics of electron transfer. However, to understand the kinetics of MAE, we need to understand not only the kinetics of electron transfer but also the response of the electrons in the metal nanoparticle that leads to a vacancy being produced in the Si valence band, i.e. hole injection.
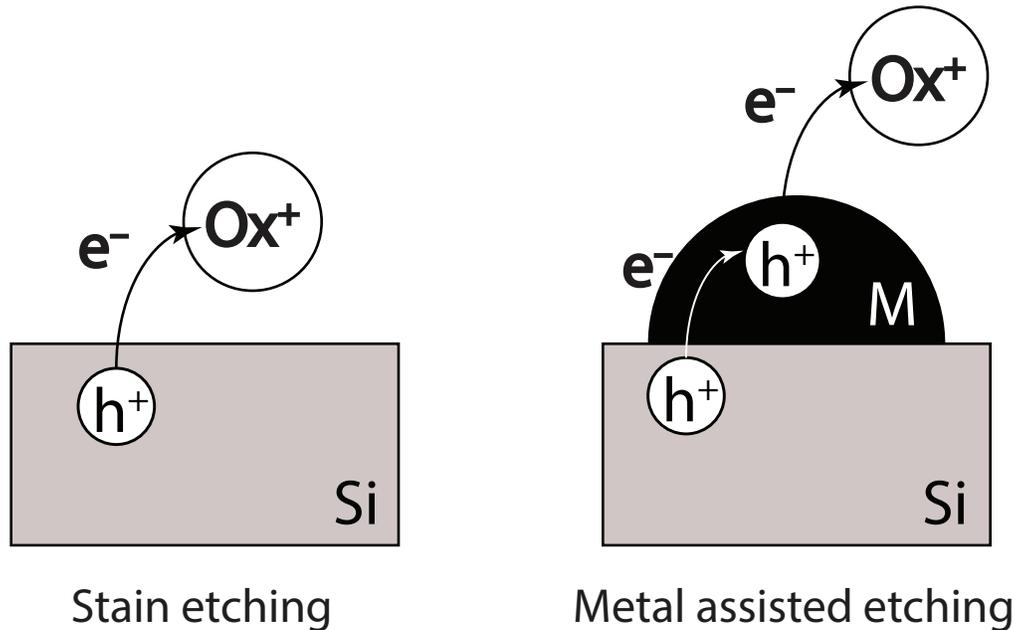

Figure 1. An electron e^- is transferred to initiate (a) stain etching and (b) metal-assisted etching. The electron is transferred to a solution phase oxidant, Ox^+. The resulting hole h^+ is injected directly into Si in the case of stain etching. In metal assisted etching, an electron must be removed from the Si, pass through the metal M *en route* to the oxidant in order to create a hole in the Si valence band.

Few extensive quantitative studies of MAE have been made. Three important studies in this regard are those of Chartier et al [21], Chiappini et al [22] and Kolasinski et al [23]. For stain etching, the only investigation of the stoichiometry of etching is the study of Kolasinski and Barclay [24]. In the latter two studies not only was gravimetric analysis used to measure the extent of Si etching; but also, the production of H_2 and the consumption of the oxidant were also monitored.

Chartier et al [21] studied MAE in the presence of H_2O_2 as an oxidant and Ag as the catalyst. The Ag nanoparticles were deposited at low densities, so that no dendrites were formed, which are known to favor the production of Si nanowires [10]. They emphasized the role of the oxidant concentration in determining the etch rate and etching regime. They proposed that the oxidant concentration plays the role of a control parameter similar to the current density in anodic porous silicon formation. Thus, just as there is a critical current density j_{ps} below which

por-Si can be formed and above which electropolishing occurs, so too must there be an electroless etch rate above which polishing should occur. They proposed that the ratio of HF to H_2O_2 should be seen as a control parameter in the form

$$\rho = \frac{[HF]}{[HF]+[H_2O_2]} \quad . \tag{1}$$

Gravimetric analysis and scanning electron microscopy to measure pore depth were used to quantify etching and etch rates. The penetration of catalyst particles was a maximum when $\rho \approx 0.85$, while the etch rate is maximized at $\rho \approx 0.45$. Four domains of structure formation were observed. In the range $0.7 \leq \rho \leq 1$, etch track pores with a diameter close to those of the Ag nanoparticle were formed. For $0.2 \leq \rho \leq 0.7$, cone shaped macropores surrounded by microporous silicon are found. For $0.09 \leq \rho \leq 0.2$, craters with diameters of several micrometers were observed. Below $\rho = 0.09$, polishing was observed.

Chiappini et al [22] performed extensive studies of MAE with H_2O_2 used as the oxidant and deposits of either Ag or Au as the catalyst. Little difference was found in the etch rate between the two metals. The rate of etching responds sensitively to oxidant concentration, consistent with the results of Chartier et al [21]. The structure of the etched layers also responds to the oxidant concentration with a relatively higher concentration of H_2O_2 resulting in higher porosity and larger pores. As has been noted by many other authors [6-8,25], five distinguishable morphologies result from MAE: solid nanowires, porous nanowires, porous nanowires on top of a porous silicon film, porous silicon films and polished/roughened silicon surfaces. The key parameters controlling the resulting morphology are silicon resistivity, H_2O_2 concentration, metal employed and concentration of ethanol added as a surfactant. HF concentration influences the etch rate but not morphology. These same nanostructures can be obtained under comparable conditions employing n-type or p-type Si indicating that doping *type* does not play a significant role in determining the type of nanostructures that can be obtained, which has also been noted by Geyer et al [26] for etching with lithographically patterned metal films in place of metal nanoparticles.

Pores roughly the size of the metal nanoparticles are called etch track pores. Often a metal nanoparticle is found at the bottom of such pores in cross sectional images. The observation of etch track pores (equivalently nanowire formation), mesoporous silicon formation away from the etch track pores and polishing requires that more than one type of etch mechanism is occurring and that etching both local to the metal nanoparticle and remote from the nanoparticle must be explained. Etch track pores are consistent with local polishing analogous to electropolishing confined to the near-metal-nanoparticle region. At sufficiently high oxidant concentration, this will switch over to rough polishing of the entire surface, not just the etch track [21].

The formation of mesoporous silicon away from etch track pores (equivalently porous nanowires) is often attributed to the diffusion of holes into the Si substrate away from the metal nanoparticle in which they originated [6,7,15,21,27]. Qu et al [28] Chiappini et al[22] and Geyer et al [26,29] have suggested that secondary deposition of Ag ions is responsible for the remote formation of mesoporous silicon. However, metal dissolution and redeposition is not evident for Au and Pt [30] when HOOH is used as the oxidant; nonetheless, these combinations lead to the remote formation of mesoporous silicon. Furthermore, Kolasinski et al [23] have used VO_2^+ as an oxidant to form etch track pores and mesoporous Si in the presence of Ag, Au and Pt. Because of the lower electrochemical potential of VO_2^+, application of the Nernst equation shows that Au cannot be dissolved and Pt can only be minimally dissolved when VO_2^+ is used as the oxidant. Therefore, dissolution and redeposition of Ag may be involved in remote mesoporous Si formation but it is not a general mechanism that is applicable to all metals and oxidants.

Kolasinski and Barclay [24] and Kolasinski et al [23] have made quantitative studies of the stoichiometry and etch rate of stain etching [24] and MAE [23]. They have shown that H^+ reduction is inconsequential because it cannot compete with oxidant reduction. This is an example of a thermodynamically allowed process that is completely overwhelmed by a kinetic disadvantage. This result is predicted by application of Marcus theory to the rate of electron transfer from Si to oxidants, which will be treated more fully below. They have also shown that, analogous to anodic Si etching, there are three etching reactions that need to be considered: valence 2 mesoporous Si formation (analogous to the current doubling pathway), valence 4 mesoporous Si formation (analogous to the current quadrupling pathway), and valence 4 polishing (valence 4 oxide formation followed by HF stripping of the oxide) [31-33]. To distinguish these three pathways they will be called the current doubling, current quadrupling and polishing pathways. They have found that the balance between these reactions, when VO_2^+ is used as an oxidant, depends on the metal. Ag and Au follow primarily the valence 2 pathway. Pt follows primarily the valence 4 mesoporous Si formation pathway. Pd follows primarily the valence 4 polishing pathway. The valence 4 polishing pathway occurs locally below the metal nanoparticle in all cases; however, only in the case of Pd is it the predominate pathway for removal of Si atoms. The etch rate was the same within experimental uncertainty for all metals because the rate was diffusion limited under the chosen conditions.

Other groups have proposed that the rate of metal assisted etching is metal dependent. For example, Yae et al [34] have shown that the Si dissolution rate increased in the order from Ag, Au, Pt, Pd, to Rh for etching in oxygenated HF. The observed etch rates were over 4 orders of magnitude smaller than the rates in conventional MAE, thus a greater sensitivity to the metal as compared to the studies of Kolasinski et al is not surprising. Asoh et al [35] reported etch rate

depended on metal in the order Au < Pt ≤ PtPd; however, these results were based on single data points for each metal with no indication of the uncertainty in any of these points.

2. Hole Injection During Stain and Metal-Assisted Etching

It is commonly proposed [6,7,15,27] that electron transfer from Si to the oxidant is facilitated directly by the metal nanoparticle. That is, a hole is injected into the metal by electron transfer from the metal to the oxidant. The hole then diffuses to the metal/Si interface and enters the Si valence band. Once the hole is present in the Si valence band, it initiates electrochemistry along one or more of the three electrochemical pathways mentioned above (i.e. the current doubling, current quadrupling and polishing pathways). Near the metal polishing occurs and etch track pores result. Holes that diffuse more deeply into the Si lead to por-Si formation by either divalent or tetravalent etching. Charge transfer from oxidant to metal to Si leads to both local and nonlocal etching in this model.

To test the above model, we need more information about the metal/Si interface, in particular, we need to know how the bands in the metal and Si align, and how this alignment changes with different metals. Calculations of the band alignment have been made by Kolasinski [36], who has also discussed the dynamics of hole injection and transport. Electron transfer into the metal often occurs close to the Fermi energy E_F. Even if it does not, relaxation of hot holes is an ultrafast process that occurs on the femtosecond time scale. Hot holes travel no more than a few nanometers before they relax to E_F. Therefore, few if any hot holes will arrive at the metal/Si interface. Furthermore, the transfer of electrons and holes across the metal/Si interface is influenced by band bending, which also affects whether there is any driving force for injection of holes into Si or whether hole injection only occurs by random walk diffusion.

Ideal Schottky barrier heights ($E_{b,n}^{\mathrm{ideal}}$ and $E_{b,p}^{\mathrm{ideal}}$ for n-type and p-type Si, respectively) and band positions in the absence of formation of surface states and reconstruction at the interface can be calculated according to the Schottky-Mott relationships [3,37,38] found in Eqs. (2–7)

$$E_{b,n}^{\mathrm{ideal}} = \Phi_\mathrm{M} - \chi_\mathrm{S} \tag{2}$$

$$E_{b,p}^{\mathrm{ideal}} = \chi_\mathrm{S} + E_\mathrm{g} - \Phi_\mathrm{M} \tag{3}$$

$$E_{\mathrm{vac}}(z) = E_{\mathrm{vac,Si\,bulk}} + \Phi_D(z) \tag{4}$$

$$E_\mathrm{C}(z) = E_{\mathrm{vac,Si\,bulk}} - \chi_\mathrm{S} + \Phi_D(z) \tag{5}$$

$$E_\mathrm{V}(z) = E_{\mathrm{vac,\,Si\,bulk}} - \chi_\mathrm{S} - E_g + \Phi_D(z) \tag{6}$$

$$\Phi_D(z=0) = \Phi_D = \Phi_M - \Phi_S \tag{7}$$

Φ_M is the metal work function, χ_s is the Si electron affinity, and E_g is the Si bandgap. $E_{vac}(z)$ is the vacuum energy in Si as a function of the distance from the interface z. $E_{vac, \text{Si bulk}}$ is the constant value of E_{vac} deep in the Si bulk. $\Phi_D(z)$ is the value of band bending, which ranges from zero in the bulk to a maximum of Φ_D at the interface. The shape of the space charge layer for convenience is approximated by a simple exponential function to smoothly connect the limiting values at the interface and in the bulk. The Fermi energy is used as the origin, $E_F = 0$. The values of these parameters are found in [3]. Two typical band diagrams are shown in Fig 2.

Band bending and the energy of the Si valance band at the interface are the important parameters not the magnitude of the Schottky barrier. This is because a hole must be transferred from the metal to the Si valence band to induce etching. The Schottky-Mott analysis allows us to calculate the energy of the Si valence band maximum at the interface, which is labeled E in Fig. 2. An interesting aspect of the Schottky-Mott analysis is that since according to Eq. (7) the surface dipole Φ_D is given by the difference in work functions, the position of the valence band maximum at the metal/Si interface is independent of whether the material is n-type or p-type doped. To prove this, note that the energetic origin in Fig. 2 is the Fermi energy, $E_F = 0$. Therefore, the vacuum energy of bulk Si is equal to its work function $E_{vac, \text{Si bulk}} = \Phi_S$. Substituting the appropriate values for Φ_D and $E_{vac, \text{Si bulk}}$ into Eq. (6) we obtain for n-type and p-type Si, respectively,

$$E_V^n(z=0) = \Phi_S^n - \chi_S - E_g + \Phi_M - \Phi_S^n = \Phi_M - \chi_S - E_g \tag{8}$$

$$E_V^p(z=0) = \Phi_S^p - \chi_S - E_g + \Phi_M - \Phi_S^p = \Phi_M - \chi_S - E_g. \tag{9}$$

Therefore, *within the assumptions of the Schottky-Mott analysis, the valence band maximum is independent of doping type at the metal/Si interface*. This may explain the insensitivity of metal assisted etching to doping type as observed [22,26].

The Schottky-Mott analysis does not consider the presence of surface states. Surface states are electronic states that are localized spatially at the metal/semiconductor interface and energetically in the semiconductor band gap. A surface state located between E and E_F (see Fig. 2) can lower the Schottky barrier height and is, therefore, important for the performance of a biased device. Ag/Si interfaces behave close to ideally and are free of interferences from surface states, the other metals do not act as ideally. The introduction of electron trap states at the metal/Si interface would tend to localize charge at that interface. However, the presence of such trap states will not alter the fact that the Fermi energy lies above the valance band maximum in

bulk Si and will not introduce any new effects to the etch mechanism beyond what is discussed here within the confines of the Schottky-Mott analysis.

Calculations of band bending at the metal/Si interface shown in Fig. 2 demonstrate that it is energetically unfavorable for holes to diffuse away from the Ag/Si interface (as well as for Al and Cu) and into the bulk Si and that for metals such as Au, Pd and Pt, there is no driving force other than standard random walk diffusion [36].
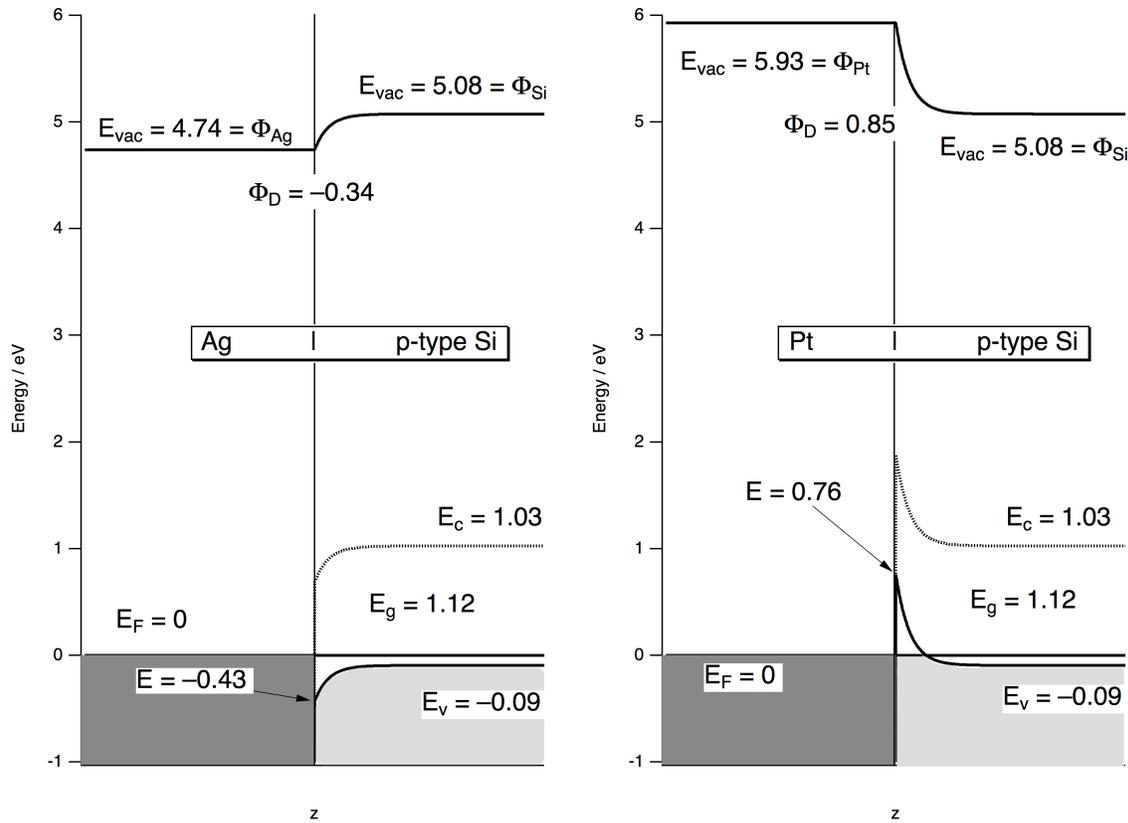

Figure 2. Band bending diagrams for Ag/Si and Pt/Si interfaces. The direction of band bending changes for low work function metals such as Ag, Cu and Al between n-type and p-type Si. For high work function metals such at Pt and Pd, band bending is upward on both n- and p-type Si. Band bending is also always upward for Au but the valence band position of Si at the interface is just $E = 0.14$ eV. E_{vac} = the vacuum energy. Φ_M = metal work function. Φ_{Si} = Si work function. E_g = Si band gap. E_F = Fermi energy. E_C = Si conduction band energy. E_V = Si valence band energy. Φ_D = maximum band bending. The value E indicates the energy of the Si valence band directly at the metal/Si interface. $E_{b,p}^{ideal}$ is the Schottky barrier height from Eq. 3.

Inspection of Fig. 2 reveals that Ag corresponds to the common perception of band bending at the metal/Si interface: Bands bend upward in n-type Si and downward in p-type Si. This relationship also holds for the two most common metals used as interconnects in semiconductor circuits, namely, Al and Cu. However, this behavior is a reflection of the work

functions of these metals compared to the work functions of n-type and p-type Si. It does not describe universal behavior. For higher work function metals, such at Au, Pd and Pt, the bands bend upward for both p-type and n-type material.

Several groups, for instance [12,22,26,28,29], have noted that Ag$^+$ may take part directly in the charge transfer that leads to Si etching. There are strong indications for Ag$^+$ dissolution with subsequent redeposition. Figure 2 demonstrates that because of the low work function of Ag, *a hole injected into Ag is more stable in the metal nanoparticle than it is in Si*. Therefore, the injected hole is available to form Ag$^+$. If redeposition were to occur away from the metal nanoparticle that released the ion, this pathway would lead to nonlocal etching. Metal oxidation and redeposition have been proposed to account for all [28] or at least a portion of the charge transfer that leads to etching [22,26,29]. Particularly strong evidence for the role played by redeposition was found in the observation [22] that formation of por-Si occurred on wafers without deposited Ag when these wafers were placed in the same solution as the Ag-deposited wafers either during the metal-assisted etch or after completion of an etch of a Ag-deposited wafer. However, no porosification occurs on blank wafers in H$_2$O$_2$ + HF solution if that solution has not first been exposed to a wafer with deposited Ag.

Dissolution and redeposition, however, cannot be the only cause of nonlocal etching. One problem with ascribing all of the nonlocal etching to Ag$^+$ redeposition is that, as will be shown in the next section, Marcus theory tells us that the rate of redeposition of Ag$^+$ on Ag nanoparticles will be order of magnitude faster than on bare Si. This has been confirmed experimentally by Kolasinski et al [23,24].

While band bending is favorable for dissolution of Ag, Fig. 2 demonstrates that for ideal interfaces of Au, Pd and Pt with Si there is no barrier to transport of holes across the M/Si interface. There also is no driving force to push them across the interface since all of the hole states above E_F in the Si are already "occupied", which effectively makes the interface metallic. Nonetheless, band bending presents a barrier that prevents the holes from leaving the space charge layer. Calculation of the space charge layer width W as a function of the doping density N_D according to [37]

$$W = \sqrt{\frac{2\varepsilon_S}{eN_D}\left(V_{bi} - \frac{2k_BT}{e}\right)} \tag{10}$$

where ε_s is the permittivity of Si, e is the elementary charge, $V_{bi} = (k_BT/e)\ln(N_D/n_i)$ is the built-in potential, k_B is the Boltzmann constant, T the temperature, e is the elementary charge and n_i is the intrinsic density of donors in Si, show that the space charge layer width varies from 1.8 μm to 9.1 nm for doping densities of ranging from 10^{14} to 10^{19} cm^{-3}, see Fig. 3.
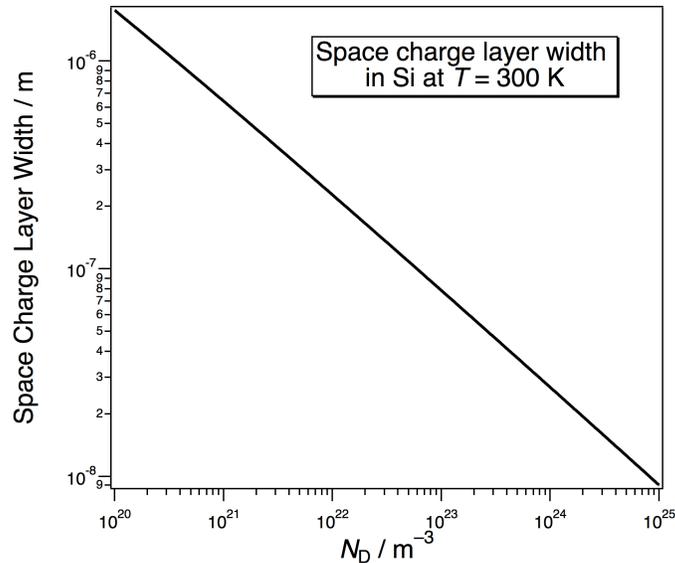
Figure 3. The calculated space charge layer width W is shown as a function of the doping density N_D for Si at $T = 300$ K.

Chiappini et al [22] observed a mesoporous Si film with a thickness of several μm on a highly (10^{19} cm^{-3}) doped substrate. This is orders of magnitude larger than the $\approx$10 nm space charge layer width to which directly injected holes are confined. There is no evidence for redeposition of Au, Pd and Pt [30] when H_2O_2 is used as the oxidant but there is evidence of mesoporous Si formation for both Au and Pt [22,25,27,30,39,40]. The oxidant VO_2^+ has a reduction potential of only 0.991 V. Therefore it cannot dissolve Au and it can only lead to negligible dissolution of Pt when it is used as the oxidant. Nonetheless, VO_2^+ can be used to induce both local and nonlocal etching with Ag, Au and Pt [23,41]. In addition, both Ag and Au exhibit the same stoichiometry indicating that etching induced by them is dominated by the current doubling pathway. It appears either (1) that dissolution and redeposition do not play a kinetically significant role, or (2) that dissolution and redeposition do not alter the mechanism of the etching processes and are not essential for local and nonlocal etching.

Could there be another means of producing nonlocal etching? It has been proposed [36] that holes build up on the metal nanoparticle. The accumulated charge polarizes the Si to affect electrochemistry just as does a bias applied from a power supply. Near the metal nanoparticle where the polarization is highest, etching is pushed into the polishing regime. Far from the nanoparticle, as the polarization drops off, etching proceeds via either the divalent or tetravalent etch pathways and mesoporous Si is formed. The model in some way is semantic: a hole injected by electron transfer to the oxidant induces a hole that initiates etching. However, without the presence of a field, there is no means of transporting the hole out of the space charge layer. Mediation of the hole injection by a field allows the induced hole to appear far from the metal/Si

interface. The field is generated by a quasi-steady-state charge imbalance on the nanoparticle maintained by the rate of electron transfer and the rate of hole consumption by etching.

Experiments [23] examining the rate and stoichiometry of metal-assisted catalytic etching have confirmed that both divalent and tetravalent etching pathways can contribute to etching. Etching in the presence of metal nanoparticles is accelerated to the point of being diffusion limited. Differences in the metal chosen do not lead to significant difference in the etch rate but they do lead to subtle differences in the balance between the different etch pathways as well as the structure of the material formed. These differences may well be related to differences in the band structure imposed by the specific metal chosen. Differences in the etched material depend on doping density but not doping type. These observations may be explained by the results obtained in the calculations represented in Fig. 2. What does not change with doping type is the position of the valence band maximum at the metal/Si interface. What does change is the space charge width (and therefore region of confinement of holes in proximity of the metal nanoparticle) as well as the polarizability of the Si.

3. Quantitative Treatment of Electron Transfer in Stain and Metal-Assisted Etching

Marcus [42-44], with primary focus on homogeneous processes, and Gerischer [45-47], with primary focus on heterogeneous processes, concurrently laid out the foundations of a theory of interfacial electron transfer. Lewis and co-workers revisited these foundations to make significant advances in our understanding of interfacial electron transfer [48-57]. Developments in the field and open questions have been elegantly reviewed by Fletcher [58].

An understanding of heterogeneous electron transfer is greatly facilitated by recognition of the following fundamental idea. Electron transfer does not occur between states that are degenerate in electronic energy. Instead, electron transfer occurs between donor and acceptor states – $|\mathrm{D}\rangle$ and $|\mathrm{A}\rangle$, respectively – of equal Gibbs energy after rearrangement of the solvation shells about the acceptor and donor. The distinction is important because only then can the dynamics be properly described. Electron transfer occurs *after* the attainment of a transition state in which the electron to be transferred is degenerate either in the acceptor or the donor species.

There are two system-dependent parameters of primary importance for determining the electron transfer probability per collision. The first is the reorganization energy λ, which is the Gibbs energy required to take the acceptor from its equilibrium solvation shell geometry to the geometry of the equilibrium solvation shell of the donor. The second is the coupling matrix element $H_{\mathrm{DA}} = \langle \mathrm{D}|\hat{H}|\mathrm{A}\rangle$ between the donor and acceptor levels. The nature of the orbitals involved in electron transfer determines the magnitude of H_{DA}. In the weak-coupling limit, the Gibbs energy curves of the reactants and products maintain their diabatic nature and the curves intersect. As the coupling grows stronger, the crossing becomes avoided. The curves split into an

excited state and an adiabatic ground state that smoothly connects the reactants through the transition state to the products.

Marcus theory quantitatively describes electron transfer occurring via an outer sphere mechanism. This corresponds to the limit of a nonspecifically adsorbed oxidant interacting with a solid surface. Kolasinski et al [59] have shown that electron transfer from Si to oxidants such as VO_2^+, Fe^{3+}, Ce^{4+} and $IrCl_6^{2-}$ are well described by Marcus theory during stain etching. The reduction of H_2O_2 is catalyzed by a metal. It is likely that electron transfer in this case is closer to the limit of an inner sphere process, though this remains to be proven. Orbital overlap is required for electron transfer, which leads to a strong distance dependence characterized by a range parameter $\beta \approx 0.8–1.2$ Å^{-1} [60,61]. Since the diameter of a water molecule is 2.76 Å and the radius of a typical hexaaquo transition metal ion is ~3–4 Å, then >90% of electron transfer via an outer sphere mechanism occurs by tunneling from an occupied band in the electrode (Si or metal on Si) into the acceptor level of the oxidant as it collides with the surface and moves from a distance of about 6 Å away from the surface (the distance of the solvated ion core with an intervening water molecule) to 3 Å (the minimum distance of the ion core from the surface).

The discussion of electron transfer rates can be made quantitative by formulating the rate constant for heterogeneous electron transfer k_{et} quantum mechanically within the framework of transition state theory as done by Marcus [43,60], Gerischer [47] and Lewis [48,50,53]. The rate constant is

$$k_{et} = \frac{2\pi}{\hbar}|H_{DA}|^2 \left(4\pi\lambda k_B T\right)^{-1/2} \exp\left(-\Delta^{\ddagger}G / k_B T\right) \tag{11}$$

where $\hbar$ is the reduced Planck constant, k_B is the Boltzmann constant, T the absolute temperature and $\Delta^{\ddagger}G$ the Gibbs activation energy for electron transfer.

Electron transfer occurs by tunneling from an occupied state at or below E_F into the not-fully-occupied acceptor level $|A\rangle$. There are several differences between electron transfer at metal and semiconductor electrodes that must be made clear. In general, the rate of electron transfer can be written

$$r_{et} = c_{red} c_{ox}\, k_{et} \tag{12}$$

where c_{red} is the concentration of the reductant (the donor D), and c_{ox} is the concentration of the oxidant (the acceptor A). Because the density of electron states at and below E_F is so large and constant, electron transfer kinetics at a metal electrode is pseudo-first-order. Thus, the rate equation becomes

$$r_{metal} = c_{ox} k_{metal} \tag{13}$$

At a semiconductor electrode the electron density is comparatively low and variable, and the rate equation is second-order

$$r_{sc} = n_s c_{ox} k_{sc}.$$ (14)

Here n_s is the density of occupied states at the band edge (the valence band since we are interested in hole injection into the valence band for catalytic etching). This means that the units of the rate constant for hole injection into a metal k_{metal} (m s^{-1}) differ from those for hole injection into a semiconductor k_{sc} (m^4 s^{-1}) [48,50].

The next major difference between electron transfer kinetics at metal electrodes and semiconductors is that *the voltage drop near a metal electrode occurs completely in the solution* because the electrons in the metal are so highly polarizable. Changing the voltage on the metal electrode changes the current because the position of the Fermi level with respect to the donor/acceptor level in the solution varies. Since this energy difference influences the activation energy for charge transfer, the current changes exponentially. On the other hand, *the voltage drop at a semiconductor electrode occurs completely in the space charge layer*. Changing the voltage does not change the positions of the band edges at the surface relative to the donor/acceptor level in solution. Instead, the current varies exponentially with applied voltage because the surface density of states changes with bias. In a similar fashion, as shown above in the band bending calculations, the polarizability of the electrons in the metal also changes the nature of the bands at the metal/semiconductor interface.

Lewis [48] demonstrated the implications of these differences for the ferrocenium/ferrocene (Fe$^{+/0}$) redox system. The difference in dielectric constant between a metal electrode such as Pt and a semiconductor such as Si is quite large. Consequently, the image charge effects in the two systems are much different [43,62] with efficient screening at a metal surface. This reduces λ_0, the inner shell contribution to λ, at a Pt electrode to about half the value found for a homogeneous electron transfer, but leaves λ_0 little changed at a Si electrode. Thus λ_0 = 0.5 eV for a Pt electrode versus 1.0 eV for a Si electrode. Using $n_{s0} = N_c \exp\left[(-0.9\text{ eV})/k_B T\right]$ with N_c = 10^{25} m^{-3} for the effective density of states in the Si conduction band, n_{s0} is 10^{10} m^{-3}, which yields $k_{sc}^{\circ} = k_{et} n_{s0} = 10^{-15} - 10^{-14}$ m s^{-1} , and exchange current densities of j_0 = 10^{-7} A m^{-2} at [Fe$^+$] = 1.0 M. The value of 0.9 eV is the magnitude of the barrier to reduction of Fe$^+$ via a conduction band process from electrons in the Si. In contrast k_{metal}° = 4 m s^{-1} for Fe$^{+/0}$ at Pt, which would lead to an exchange current density of j_0 = 4 × 10^8 A m^{-2} at [Fe$^+$] = 1.0 M. The latter value is impossibly high, as the current would first become diffusion limited. The extraordinary difference is related primarily to the reduction in the electron density in the semiconductor electrode relative to that at the metal, not to a change in mechanism. Consequently, we will

observe a substantially increased rate of electron transfer in the presence of a metal on a semiconductor surface. For example, the rate of Ag^+ deposition on metallic nanoparticles will be orders of magnitude faster than deposition on bare Si, and we should expect the etch rate during MAE to be diffusion limited regardless of which metal is chosen as long as the concentration of the oxidant is range usually used for MAE.

Within a transition state theory framework [42,48,53], the rate constant of electron transfer can be written in terms of a pre-exponential factor and a Gibbs energy of activation

$$k_{et} = A\exp\left(-\Delta^{\ddagger}G/k_B T\right). \tag{15}$$

The dimensions of A are different for a metal (m s^{-1}) and for a semiconductor (m^4 s^{-1}) as discussed above. Due to the differences in band structure, the expression for the activation energy is also different. For a metal electrode held at a potential E

$$\Delta G^{\ddagger} = \left(E - E_{ox} + \lambda\right)^2 / 4\lambda. \tag{16}$$

For a semiconductor

$$\Delta G^{\ddagger} = \left(E_V - E_{ox} + \lambda\right)^2 / 4\lambda. \tag{17}$$

E_{ox} is the Nernst potential of the oxidant, λ is the reorganization energy, and E_F or E_V is referenced to a common vacuum level along with E_{ox}. Note that the Nernst potential of the oxidant is dependent on the solution composition according to

$$E_{ox} = E^{\circ} - \frac{RT}{zF}\ln Q, \tag{18}$$

where E° is the standard reduction potential, R is the gas constant, z if the valence of the redox process, F is the Faraday constant and Q is the reaction quotient. This means that the rate of electron transfer to the oxidant depends on the solution composition not only on account of the concentration appearing in the rate equation, but also because the position of the acceptor level relative to the band from which the electron originates depends on the composition of the electrolyte. As long as the acceptor lies below the energy of the top of the band, there is no change in the electron transfer rate. However should the acceptor shift above the energy of the band, the rate will drop exponentially with increasing shift. Rarely is the extent of reaction, the volume of etchant, the total number of moles oxidant consumed, or the potential for change in the oxidant concentration mentioned in the experimental description of MAE. *This factor has the potential to lead to major issues in reproducibility and control of MAE.*

As long as the acceptor level $|A\rangle$ approaches the donor level $|D\rangle$ from above, that is, from a higher energy, electron transfer occurs either at the Fermi level for a metal or else the appropriate band edge for a semiconductor after the acceptor level has fluctuated to an appropriate energy to facilitate degenerate electron transfer [42,45,46]. In this case, all holes are injected into the electrode in a narrow energy range at E_F, the valence band maximum or conduction band minimum regardless of the ground state energy of the acceptor level on the oxidant. If the acceptor level lies below the energy of an *occupied* band, there are always states that are degenerate with respect to electronic energy available for electron transfer from the electrode. Nonetheless, the solvation shell still needs to reorganize; therefore, there is still an activation energy that must be overcome before electron transfer can occur.

4. Conclusion

In order to understand the kinetics of charge transfer during stain etching and metal assisted etching it is essential to consider the effects of band bending. The kinetics can be framed quantitatively by application of Marcus theory. The calculations and results reviewed here show that there are dramatic differences in electron transfer rates at metal and semiconductor interfaces. Electron transfer is inherently faster at metal electrodes. This is at the heart of why the metal catalyzes etching in metal assisted etching. It also militates against the role of metal ion deposition being kinetically significant on Si surfaces when metal surfaces are available for deposition. Hole injection from the oxidant to Si is direct in the case of stain etching. The metal mediates hole injection in the case of metal assisted etching. On the basis of band bending calculations, diffusion of holes away from low work function metals such as Ag is not possible. Similarly diffusion of holes outside of the space charge layer is not possible for high work function metals such as Au, Pd and Pt. Direct injection may be important to explain etch track pore formation in the immediate vicinity of the metal. However, this cannot explain etching remote from the metal. It has been proposed that the charge imbalance on (or immediately adjacent to) the metal acts to polarize the surrounding Si. This second mechanism is implicated in nonlocal etching of Si during metal assisted etching.

References

[1]   Canham L T, in *Handbook of Porous Silicon*, edited by Canham L T (Springer Verlag, Berlin, 2014), pp. 3-9.

[2]   Kolasinski K W, in *Handbook of Porous Silicon*, edited by Canham L T (Springer Verlag, Berlin, 2014), pp. 35-48.

[3]   Kolasinski K W, in *Nanostructured Semiconductors: From Basic Research to Applications*, edited by Granitzer P and Rumpf K (Pan Stanford Publishing, Singapore, 2014), pp. 45-84.

[4]   Kolasinski K W 2005 *Curr. Opin. Solid State Mater. Sci.* **9** 73-83

[5]   Loni A, Barwick D, Batchelor L, Tunbridge J, Han Y, Li Z Y and Canham L T 2011 *Electrochem. Solid State Lett.* **14** K25-K27

[6]   Huang Z, Geyer N, Werner P, de Boor J and Gösele U 2011 *Adv. Mater.* **23** 285-308

[7]   Li X L 2012 *Curr. Opin. Solid State Mater. Sci.* **16** 71-81

[8]   Levy-Clement C, in *Handbook of Porous Silicon*, edited by Canham L T (Springer Verlag, Berlin, 2014), pp. 49-66.

[9]   Chiappini C, in *Handbook of Porous Silicon*, edited by Canham L T (Springer Verlag, Berlin, 2014), pp. 171-86.

[10]   Peng K-Q, Yan Y-J, Gao S-P and Zhu J 2002 *Adv. Mater.* **14** 1164-7

[11]   Peng K-Q and Zhu J 2003 *J. Electroanal. Chem.* **558** 35-9

[12]   Peng K-Q, Yan Y-J, Gao S-P and Zhu J 2003 *Adv. Func. Mater.* **13** 127-32

[13]   Peng K-Q, Zhang M L, Lu A J, Wong N B, Zhang R Q and Lee S T 2007 *Appl. Phys. Lett.* **90** 163123

[14]   Zhang M-L, Peng K-Q, Fan X, Jie J-S, Zhang R-Q, Lee S-T and Wong N-B 2008 *J. Phys. Chem. C* **112** 4444-50

[15]   Peng K-Q, Lu A J, Zhang R Q and Lee S T 2008 *Adv. Func. Mater.* **18** 3026-35

[16]   Huang Z P, Zhang X X, Reiche M, Liu L F, Lee W, Shimizu T, Senz S and Gösele U 2008 *Nano Lett.* **8** 3046-51

[17]   Huang Z P, Shimizu T, Senz S, Zhang Z, Zhang X X, Lee W, Geyer N and Gösele U 2009 *Nano Lett.* **9** 2519-25

[18]   Scheeler S P, Ullrich S, Kudera S and Pacholski C 2012 *Nanoscale Res. Lett.* **7** 450

[19]   Kolasinski K W, Mills D and Nahidi M 2006 *J. Vac. Sci. Technol. A* **24** 1474-9

[20]   Mills D and Kolasinski K W 2004 *J. Vac. Sci. Technol., A* **22** 1647-51

[21]   Chartier C, Bastide S and Levy-Clement C 2008 *Electrochim. Acta* **53** 5509-16

[22]   Chiappini C, Liu X W, Fakhoury J R and Ferrari M 2010 *Adv. Func. Mater.* **20** 2231-9

[23]   Kolasinski K W, Barclay W B, Sun Y and Aindow M 2015 *Electrochim. Acta* **158** 219-28

[24]   Kolasinski K W and Barclay W B 2013 *Angew. Chem., Int. Ed. Engl.* **52** 6731-4

[25]   Tsujino K and Matsumura M 2005 *Electrochem. Solid State Lett.* **8** C193-C5

[26]   Geyer N, Fuhrmann B, Leipner H S and Werner P 2013 *ACS Appl. Mater. Interfaces* **5** 4302-8

[27]   Chattopadhyay S, Li X and Bohn P W 2002 *J. Appl. Phys.* **91** 6134-40

[28]   Qu Y Q, Liao L, Li Y J, Zhang H, Huang Y and Duan X F 2009 *Nano Lett.* **9** 4539-43

[29]   Geyer N, Fuhrmann B, Huang Z P, de Boor J, Leipner H S and Werner P 2012 *J. Phys. Chem. C* **116** 13446-51

[30]   Li X and Bohn P W 2000 *Appl. Phys. Lett.* **77** 2572-4

[31]   Lehmann V, *Electrochemistry of Silicon: Instrumentation, Science, Materials and Applications*. (Wiley-VCH, Weinheim, 2002).

[32]   Kolasinski K W 2003 *Phys. Chem. Chem. Phys.* **5** 1270-8

[33]   Kolasinski K W 2009 *Surf. Sci.* **603** 1904-11

[34]   Yae S, Morii Y, Fukumuro N and Matsuda H 2012 *Nanoscale Res. Lett.* **7** 352

[35]   Asoh H, Arai F and Ono S 2009 *Electrochim. Acta* **54** 5142-8

[36]   Kolasinski K W 2014 *Nanoscale Res. Lett.* **9** 432

[37]   Sze S M, *Physics of Semiconductor Devices*, 2nd ed. (John Wiley & Sons, New York, 1981).

[38]   Tung R T 2014 *Applied Physics Reviews* **1** 011304

[39]   Chattopadhyay S and Bohn P W 2004 *J. Appl. Phys.* **96** 6888-94

[40]   Harada Y, Li X, Bohn P W and Nuzzo R G 2001 *J. Am. Chem. Soc.* **123** 8709-17

[41]   Kolasinski K W and Barclay W B 2013 *ECS Trans.* **50** 25-30

[42]   Marcus R A 1965 *J. Chem. Phys.* **43** 679-99

[43]   Marcus R A 1990 *J. Phys. Chem.* **94** 1050-5

[44]   Marcus R A 1991 *J. Phys. Chem.* **95** 2010-3

[45]   Gerischer H 1960 *Z. Phys. Chem. N. F.* **26** 233-47

[46]   Gerischer H 1961 *Z. Phys. Chem. N. F.* **27** 40-79

[47]   Gerischer H, in *The CRC Handbook of Solid State Electrochemistry*, edited by Gellings P and Bouwmeester H (CRC Press, Boca Raton, 1997), pp. 9-73.

[48]   Lewis N S 1991 *Annu. Rev. Phys. Chem.* **42** 543-80

[49]   Pomykal K E, Fajardo A M and Lewis N S 1996 *J. Phys. Chem.* **100** 3652-64

[50]   Royea W J, Fajardo A M and Lewis N S 1997 *J. Phys. Chem. B* **101** 11152-9

[51]   Fajardo A M and Lewis N S 1997 *J. Phys. Chem. B* **101** 11136-51

[52]   Royea W J, Fajardo A M and Lewis N S 1998 *J. Phys. Chem. B* **102** 3653

[53]   Lewis N S 1998 *J. Phys. Chem. B* **102** 4843-55

[54]   Gao Y Q, Georgievskii Y and Marcus R A 2000 *J. Chem. Phys.* **112** 3358-69

[55]   Gstrein F, Michalak D J, Royea W J and Lewis N S 2002 *J. Phys. Chem. B* **106** 2950-61

[56]   Lewis N S 2005 *Inorg. Chem.* **44** 6900-11

[57]   Hamann T W, Gstrein F, Brunschwig B S and Lewis N S 2005 *J. Am. Chem. Soc.* **127** 13949-54

[58]   Fletcher S 2010 *J Solid State Electrochem.* **14** 705-39

[59]   Kolasinski K W, Gogola J W and Barclay W B 2012 *J. Phys. Chem. C* **116** 21472–81

[60]   Marcus R A and Sutin N 1985 *Biochim. Biophys. Acta* **811** 265

[61]   Barbara P F, Meyer T J and Ratner M A 1996 *J. Phys. Chem.* **100** 13148-68

[62]   Smith B B and Koval C A 1990 *J. Electroanal. Chem.* **277** 43-72